

EFSUMB



EFSUMB – European Course Book

Editor: Christoph F. Dietrich

Ultrasound of the pancreas

**Mirko D’Onofrio¹, Valentina Ciaravino², Vlastimil Valek³, Alessandro Beleù¹, Christian
Jensen⁴, Riccardo De Robertis⁵**

¹Department of Radiology, GB Rossi University Hospital, Verona, Italy

²Department of Radiology, Morgagni Pierantoni Hospital, Forlì, Italy

³Department of Radiology and Nuclear Medicine, University Hospital Brno and Medical Faculty,
Masaryk University Brno

⁴Klinik für Innere Medizin, Krankenhaus Märkisch Oderland, Strausberg; Brandenburg Institute for
Clinical Ultrasound (BICUS) at Medical University Brandenburg, Neuruppin, Germany

⁵Department of Radiology, Ospedale Civile Maggiore, Verona, Italy

Corresponding author:

Prof. Dr. Mirko D’Onofrio

Department of Radiology; GB Rossi University Hospital; University of Verona / Italy

Tel.: (+) +39 045 8124301;

Fax: (+) +39 045 8027490

Email: mirko.donofrio@univr.it

Topographic remarks

The pancreas is a medium retroperitoneal organ, slightly flattened and tapered. It is located transversally in front of the main vessels at the level of the first or second lumbar vertebra. It is considered to be a fixed posterior organ. It presents as a slightly oblique shape extending left and upward, with the cephalic portion in a generally lower position compared with the body and the tail. It lies against the vertebral column, which determines the slight curvature of the organ, and is surrounded by soft retroperitoneal and peritoneal tissue.

Pancreas anatomy

The pancreas is a compound acinar gland. Its exocrine excretion is pancreatic juice, an important digestive fluid, while the endocrine secretion consists of peptid hormones involved mainly in sugar metabolism. The pancreas is usually divided in four parts: the head with the uncinata process, neck, body and tail. The head lies within the curve of the duodenum and appears in complete contact with the posterior abdominal wall, the inferior vena cava (IVC) and the portal vein at the top. The uncinata process originates from the lower left portion of the head and lies posterior to the superior mesenteric vessels. The neck or isthmus generally appears as a slight constriction connecting the head to the body. It is located in front of the superior mesenteric vein and is completely overlaid on its anterior surface by the posterior parietal peritoneum; its postero-inferior surface is related to the origin of the portal vein, which is formed by the junction of the superior mesenteric and splenic veins. The posterior parietal peritoneum, which overlays the front face of the pancreatic body, limits the posterior face of the lesser sac (Bursa omentalis). The pancreatic body is covered frontally by the gastric cavity, posteriorly it is in contact with the splenic vein and it is related to the superior mesenteric artery and the left renal vein, which courses between the superior mesenteric artery and the aorta to merge into the IVC. The superior margin is slightly crossed anteriorly by the splenic artery, which arises from the coeliac trunk, whereas the inferior margin lies on the duodeno-jejunal flexure. The tail is orientated posteriorly, left and upwards, it touches the splenic hilum as well as the left adrenal gland and the upper kidney. It represents the mobile part of the gland and, similar to the body, it is separated from the stomach by the lesser sac. The anteroposterior dimension of the pancreas varies greatly between individuals and tends to decrease with age. The normal

measurements are: head, 2 cm; neck < 1 cm; body and tail, 1 - 2 cm; mean length is 13 - 15cm [(1)].

Pancreatic and peri-pancreatic veins

The veins of the pancreas open into the splenic and superior mesenteric veins, from where the junction of the portal vein originates. The superior mesenteric vein runs over the uncinate process, whereas the splenic vein, rising from the splenic hilum, courses along the supero-posterior surface of the pancreas.

Pancreatic and peri-pancreatic arteries

The arteries of the pancreas derive from the splenic and the pancreaticoduodenal branches of the hepatic and superior mesenteric arteries.

The splenic artery, arising from the coeliac artery, runs along the superior margin of the gland; from it, some arteries perpendicular to the splenic artery enter the body and tail parenchyma. In 92% of cases the common hepatic artery, which courses along the superior margin of first portion of the duodenum and continues into the proper hepatic and gastroduodenal arteries, also arises from the coeliac trunk [(2)]. The gastroduodenal artery courses along its ventral surface.

The superior mesenteric artery arises from the aorta behind the lower portion of the pancreatic body then courses anteriorly to the uncinate process and the third portion of the duodenum.

Pancreatic ductal system

The pancreatic ductal system is represented by the main pancreatic duct (also known as the Wirsung duct) and the accessory, functional or not, pancreatic duct (also known as the Santorini duct).

The main pancreatic duct takes its origin from the junction of the small ducts of the tail lobules. It courses transversely from left to right through the pancreatic body and flows into the major duodenal papilla (of Vater) jointly with the common bile duct (CBD). It appears as a thin hypoechoic line bordered by two echogenic margins and its maximum diameter varies from 3 mm in young adults to 4 mm in older people in the genu pancreatis. The CBD crosses

the anterior surface of the portal vein to the right of the proper hepatic artery and runs behind the first portion of the duodenum to arrive into the parenchyma of the pancreatic head, close to the second portion of the duodenum.

The accessory pancreatic duct originates from the main pancreatic duct and just crosses the head of the pancreas, superficial to the main duct. It flows into the minor duodenal papilla, which is 2 cm higher than the major duodenal papilla.

Pancreas development

The pancreas develops in two parts, the dorsal and ventral. The dorsal part arises as a diverticulum from the dorsal side of the duodenum, just above the hepatic digression and, grows upwards and backwards into the dorsal mesogastrium forming a part of the head and the uncinata process as well as the whole body and tail.

The ventral portion appears as a diverticulum from the primitive bile duct, which forms the remaining part of the head and the uncinata process. As a consequence, the duct of the dorsal part (accessory pancreatic duct) opens independently into the duodenum, while the duct of the ventral part (main pancreatic duct) opens together with the CBD. Around the sixth week of gestation the two parts of the pancreas meet and fuse to establish a communication between their ducts. Following fusion of both ducts the terminal part of the accessory duct remains thin and its opening into the duodenum is occasionally obliterated, whereas the pancreatic duct increases in size and forms the main duct of the gland.

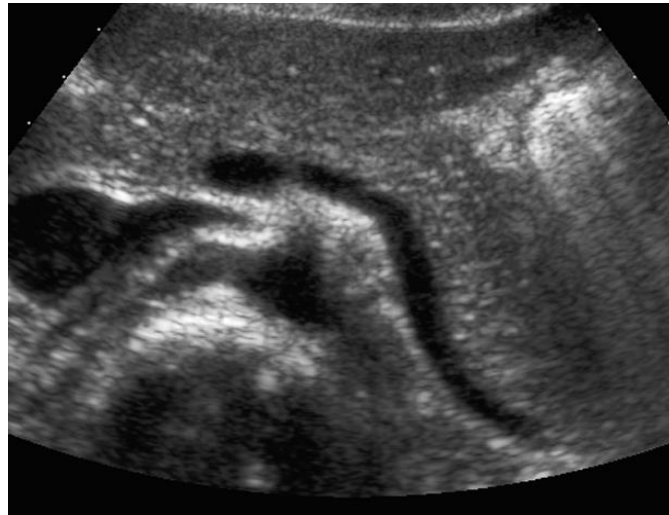
At first the pancreas is directed upwards and backward between the two layers of the dorsal mesogastrium, which gives it a complete peritoneal sheath, its surfaces facing the right and the left side. With a change in position of the stomach, the dorsal mesogastrium is drawn downward and to the left, so that the right side of the pancreas is directed backward and the left directed forwards. The right surface connects to the posterior abdominal wall and the peritoneum covering absorbed; thus, in the adult, the gland appears to lie behind the peritoneal cavity.

Knowing the physiological pancreatic embryogenesis is important to correctly recognize and evaluate some pancreatic anomalies and pseudo-lesions that potentially may occur as a result of the embryologic pancreatic fusion.

Ultrasound study of the pancreas and anatomy

The study of the pancreas includes transverse, longitudinal and angled oblique scan planes [Figure 1].

Figure 1 Oblique ultrasound scan of the pancreatic gland. The pancreatic tail, body, isthmus and the upper part of the head of the pancreas can all be visualised.



The plane passing through the emergence of the coeliac trunk identifies the beginning of body-tail. In the presence of gastric gas it can cover the left portion of the pancreatic gland. The plane passing through the splenic vein demonstrates typical “comma” morphology. In this scan, it is easy to identify the body with the pancreatic duct [Figure 2] and the isthmus of the pancreas on the confluence of the splenic vein with the superior mesenteric vein. At the level of the lateral border of the head the gastroduodenal artery is often seen ventrally represented by anechoic image; and the CBD can be seen dorsally.

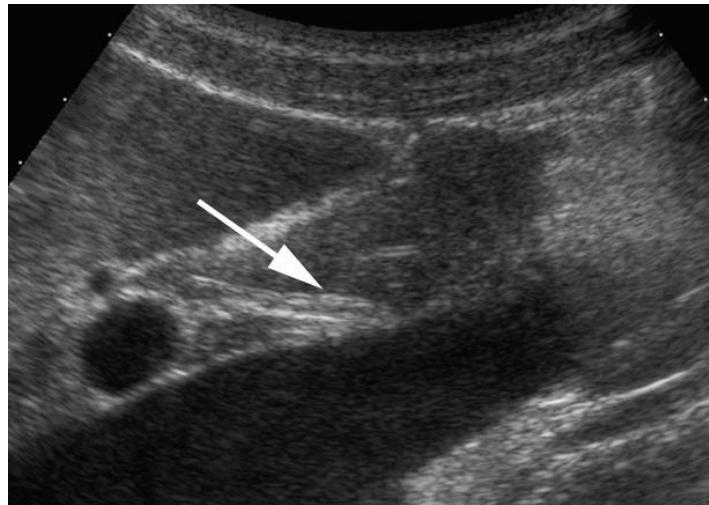
Figure 2 Pancreatic duct. Ultrasound oblique scan of the pancreatic body with visualisation of the main pancreatic duct (arrow).



The scan passing through the mesenteric vessels visualises the lower portion of the pancreatic head and the uncinata process, which is anatomically located between the superior mesenteric vein and the IVC. The superior mesenteric artery appears in front of the aorta and to the left of the superior mesenteric vein.

Longitudinal scans are executed on the four anatomical parts of the pancreas. The head is visualised in all its extensions, and in terms of its relationship with the IVC. Its cephalic portion is cranially delimited by the portal vein and the first duodenal part; more caudally it connects with the third duodenal portion. With a longitudinal and slightly oblique scan it is usually possible to visualise the intra-pancreatic CBD [Figure 3].

Figure 3 Intra-pancreatic common bile duct. Ultrasound longitudinal and slightly oblique scan of the pancreatic head with visualisation of the pancreatic duct and the intra-pancreatic tract of the common bile duct (arrow).



The scans at the neck level require the superior mesenteric vein as reference point; this is visualised at the junction with the splenic vein. Somewhat more dorsally it is possible to see the uncinate process. The main pancreatic duct can be visualised at the level of the pancreatic body [Figure 2]. The reference point on the body is represented by the splenic vessels, transversally orientated, which course on the superior border. The tail can be visualised on a longitudinal anterior scan; however, demonstration of this anatomical structure is often difficult owing to gastric gas, which can cover it. Left intercostal scans are generally used to localise the caudal portion by using the splenic acoustic window.

The normal US pancreatic echogenicity and appearance depends on patients age, due to the para-physiological changes that occur within the gland over the years. The echotexture of the normal pancreas is usually homogeneous, but a mottled appearance may sometimes be observed. In young patients there is few adipose tissue within the pancreatic gland, whereas during the years adipose tissue is collected among pancreatic lobules until a complete fatty replacement, also known as lipomatosis, of the pancreas. The normal “young” pancreas has a low echogenicity, similar to the normal liver or even more hypoechoic than the liver, whereas with aging and obesity, the more adipose tissue is collected, echogenicity is increasing. In case of severe lipomatosis the pancreatic gland may be as echogenic as the

adjacent retroperitoneal fat, occurring in up to 35% of cases [(1;3)]. Other causes of pancreatic fatty infiltration include chronic pancreatitis, dietary deficiency, viral infection, corticosteroid therapy, cystic fibrosis, diabetes mellitus, hereditary pancreatitis and obstruction caused by a stone or a pancreatic carcinoma [(4)].

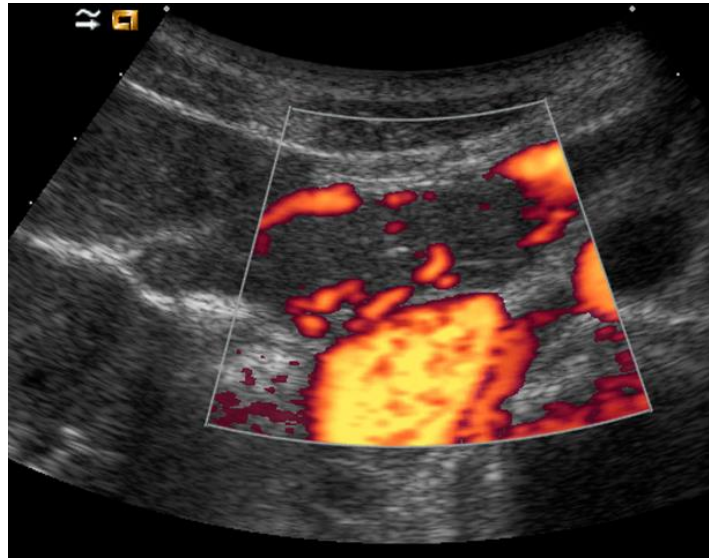
Doppler study of the pancreas and vascular anatomy

Doppler studies are an integral part of ultrasound examination of the pancreas [(5)]. The peri-pancreatic vascular structures that are evaluated and easily recognised are the portal vein, the celiac trunk, the splenic artery and vein, the gastro-duodenal artery, the superior mesenteric artery and vein, the aorta and the IVC. Only a few parenchymal vessels are usually appreciable in normal conditions; however, the visualisation of smaller peri-pancreatic [Figure 4] and intra-pancreatic [Figure 5] vessels is possible thanks to increased Doppler sensitivity.

Figure 4 Gastro-duodenal artery. Colour Doppler ultrasound longitudinal scan of the pancreatic head. The gastro-duodenal artery can be visualised.



Figure 5 Pancreatic arterial arcades. Power Doppler ultrasound transverse scan of the pancreatic head. The pancreatic arterial arcades can be visualised.



Clinical applications of the Doppler studies of peri-pancreatic vessels include the assessment of patency and features of blood flow. Doppler and pulsed Doppler appearance of peri-pancreatic vessels have been well-documented [(1;2)]. In normal conditions, the mean speed of blood in peri-pancreatic arteries is approximately $103 \pm 8\text{cm/s}$ in the coeliac trunk, $78 \pm 6\text{cm/s}$ in the hepatic artery, $85 \pm 18\text{cm/s}$ in the splenic artery and $100 \pm 22\text{cm/s}$ in the superior mesenteric artery [(1)]. Mean portal flow velocity is $12 - 20\text{cm/s}$. The resistance index in the superior mesenteric artery is in general higher than in the coeliac trunk and its branches [(1)]. Abnormal signals and physiological variations in Doppler waveform in peri-pancreatic vessels are not fully understood because of the influence of physiological, pharmacological and pathological conditions [(1)]. However, Doppler examination allows the changes produced by diseases in peri-pancreatic vessels to be recognised. This may be of importance in staging of pancreatic cancer and for the detection of vascular complications of pancreatitis.

Other ultrasound techniques

Ultrasound evaluation has different tools available to study organs, and in particular the pancreatic gland. As previously described, the ultrasound B-mode (Brightness Mode) is the

conventional ultrasonography technique. Other techniques that could be used in the pancreatic evaluation are harmonic imaging, compound and volumetric imaging, Doppler imaging, already described, elastography imaging and contrast-enhanced ultrasound (CEUS). A pancreatic harmonic examination is characterized by a higher sensitivity than conventional B-mode ultrasound regarding focal pancreatic lesions detection, both solid and cystic ones [(4-6)]; moreover this technique is able to more clearly delineate lesion margins and mass internal solid components [(7)]. Harmonic imaging, compared to B-mode ultrasound, provides a higher differentiation of soft tissue, providing both the detection of even small lesions with little changes in echogenicity in respect to the adjacent parenchyma and the identification of calcifications. Furthermore, it has the ability to better clearly study deep structures and overweight patients [(5)]. Summarizing, harmonic imaging can increase both spatial and contrast resolution, providing an enhanced overall image quality, better lesion conspicuity, and advantages in fluid-solid differentiation in the pancreatic study, compared to conventional B-mode ultrasound [(4)]. Compound imaging is able to increase contrast and spatial resolution in the B-mode imaging. Volumetric ultrasound imaging is a relatively new technique based on the acquisition of a volume dataset of anatomic structures. The correct application of these new technologies in the ultrasound pancreatic study results in a conventional imaging with very high spatial and contrast resolution. Elastography imaging allows for a non-invasive analysis of tissue stiffness, giving a new revolutionary approach in the study of focal and diffuse diseases. Pancreas elastography can be obtained by using two main techniques: first is strain elastography (SE); second is shear wave elastography (SWE), which in turn includes transient elastography (TE), point SWE, 2D-SWE and 3D-SWE, and acoustic radiation force impulse (ARFI), the most recent technique introduced [(8)]. Through a colour or a grey scale map, a qualitative evaluation of the elastic properties of tissues is provided by the strain elastography, giving the opportunity that isoechoic lesions, which are undetectable at conventional B-mode ultrasound, might be identified at elastography studies. Shear wave imaging, on the contrary, allows both qualitative and quantitative evaluations. The ARFI ultrasound technique permits the evaluation of mechanical strain properties of deep tissues without the need of external compression, allowing both a qualitative and a quantitative evaluation of the tissue stiffness: in the qualitative one it creates a static map of the relative tissues stiffness; whereas in the quantitative one the speed of the wave through the tissue is calculated in m/s and the stiffer the tissue is, the

greater the shear wave velocity [(8)]. The healthy pancreas appears as intermediately soft tissue, characterized by a homogeneous soft tissue green area at elastographic imaging; with the adipose tissue accumulation during the years and fibrosis degeneration of parenchyma, the elastographic image becomes heterogeneous, due to different colour areas within the gland. The mean wave velocity value obtained in a healthy pancreas with ARFI technique is about 1.40 m/s, as reported in literature [(8-10)].

Contrast-enhanced ultrasonography is a relatively new tool of conventional ultrasound that significantly increases the accuracy of the first line examination in characterizing focal solid and cystic lesions. Administration of ultrasound contrast agents allows an accurate evaluation of macro- and microcirculation, in and around a focal mass, giving more detailed and advanced results than color-Doppler study thanks to its high spatial, contrast and temporal resolution. Due to the rich vascular gland supply, enhancement of the pancreatic gland begins almost at the same time as aortic enhancement. After this early phase (arterial/pancreatic, from 10 seconds to 30 sec), there is the venous phase (from 30 to approximately 120 sec) and the late phase (about 120 sec after injection. Ultrasound contrast agents have a purely intravascular distribution without any interstitial phase, which is an important distinctive feature from contrast media used in CT and MRI studies [(4)].

Pancreatic pseudolesions

Pancreatic pseudolesions may be the result of changes in the volume and/or in the echogenicity of the gland. Reduction of the pancreatic volume can be observed very frequent after 40 years of age, due to a process of physiologic senile involution of the gland. Pancreatic gland atrophy is also a typical finding in patients with diabetes mellitus type 1. Conversely, an increase in pancreatic gland volume is often observed in overweight patients, in association with hepatosplenomegaly. Pancreatic echogenicity is considered normal if comparable or slightly higher than that of normal healthy liver, but often this comparison fails due to liver steatosis or because the pancreas, together with the liver, increases its echogenicity because of fatty infiltration, often observed in obese, diabetics, dysmetabolic, cystic fibrosis patients.

Pancreatic pseudo-masses may be frequently due to focal echogenicity alterations of the gland. Typical and quite common is the pseudo-mass of the pancreatic head-uncinate

process, actually supported by the lower echogenicity of the ventral pancreas compared to the dorsal pancreas, which is probably due to the different distribution of the local vasculature. Another pitfall is the presence of big pancreatic lobules (1 cm of diameter) that can alter the profile of the gland simulating neoplastic nodules [(4;11)].

Pancreatic trauma

The pancreas is injured relatively uncommon in trauma in respect to other abdominal organs, occurring in less than 2% of blunt trauma cases. This injury has to be recognized as soon as possible, due to its considerably high morbidity and mortality in cases of delayed diagnosis, incorrect classification of the injury, or delays in treatment. Moreover a blunt pancreatic injury is more common in children and young adults, due to their thinner or absent mantle of protective fat, which usually surrounds the pancreas in older adults [(12;13)]. Ultrasound can cover a first role in blunt trauma patients evaluation, doing it at patient's bedside, acquiring more importance in case of paediatric patients, due to its absence of ionizing radiations. Moreover contrast-enhanced ultrasound (CEUS) could give new important details about lesions occur in the pancreas. Ultrasound can cover an important role also in patients follow-up. Of course ultrasound examination and real-time CEUS should not be considered as a replacement for CT in all the cases [(12;14)].

Ultrasound findings could be a pancreatic localized traumatic enlargement or diffuse oedema simulating inflammatory acute pancreatitis. An important sign in trauma patients is the presence of peri-pancreatic fluids that may be a sign of pancreatic contusion [(12-15)]. It is important to try to delineate the main pancreatic duct in all cases of pancreatic injury, due to complications of trauma are most likely to occur from rupture or stenosis of this structure. Transection throughout the pancreas parenchyma is suggestive of ductal injury. Contrast agents injection could improve the detection of injured parenchymal areas.

Pancreatic diffuse inflammatory disease

Acute pancreatitis

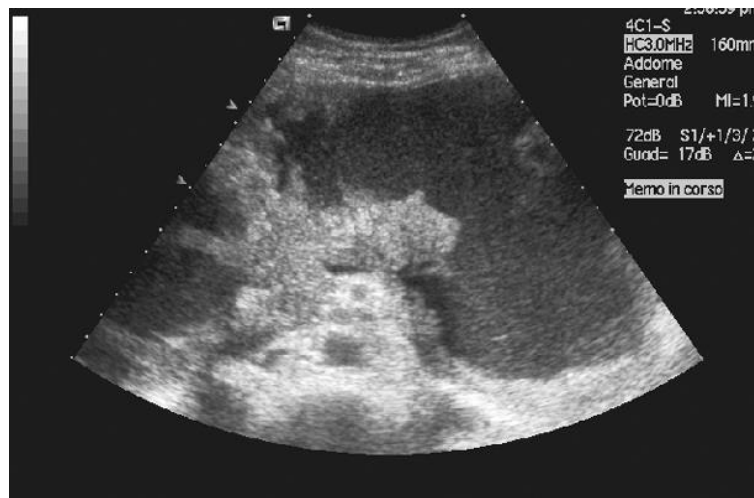
Acute pancreatitis is an acute inflammatory process of the pancreatic gland that can be of different degrees, such as mild, moderate severe and severe, according to the presence or

not of local complications or organs failure. According to the 2012 revised Atlanta classification of acute pancreatitis, acute pancreatitis is clinically defined by at least two of the following three features [(16)]: (1) abdominal pain suggestive of pancreatitis (epigastric pain that could be radiate to the back), with the start of such pain considered to be the onset of acute pancreatitis; (2) serum amylase and lipase levels three or more times normal; and (3) characteristic findings on CT, MRI imaging, or transabdominal ultrasound studies. Diagnosis is usually based on laboratory assay of serum amylase and lipase levels [(17)].

Acute pancreatitis is classified as interstitial edematous pancreatitis or necrotizing pancreatitis, in turn split in three categories depending on necrosis location (pancreatic parenchymal necrosis alone, 5%; peri-pancreatic necrosis alone, 20%; and pancreatic parenchymal necrosis with peri-pancreatic necrosis 75-80%), that can be sterile or infected [Figure 6]. Biliary stones, one of the most frequent causes of acute pancreatitis, can be detected at the time of the diagnosis, giving to ultrasound an important role to find out the trigger cause of the pancreatitis.

Acute pancreatitis can be accompanied by pancreatic parenchymal or peri-pancreatic collections: the current revision of the Atlanta classification distinguishes between fluid and non-liquefied collections [(16)]. The acute collections (within 4 weeks from symptoms onset) are referred to as either acute peri-pancreatic fluid collection (APFC) or as acute necrotic collection (ANC), depending on the absence or presence, respectively, of necrosis. After 4 weeks the collections are named respectively pseudocysts or walled off necrosis, depending on the presence of necrosis within the collections. All of these collections can be sterile or infected.

Figure 6 Necrotizing pancreatitis and pancreatic fluid collection. Ultrasound oblique scan of the pancreatic gland with visualisation of a large inhomogeneous fluid collection at the pancreatic body/tail.



Transabdominal ultrasound is usually the first imaging method for studying patients with acute abdomen due to its wide availability. However, several limitations can be present in patients with acute pancreatitis mainly related to abdominal pain, which makes probe compression very difficult, and to the presence of abundant overlying gas owing to a paralytic ileus, with the frequent result of a partial or inadequate visualization of the pancreas at the beginning of the disease. Therefore, ultrasound has a major role in excluding other causes of acute abdominal pain and for the detection of indirect signs of acute pancreatitis (e.g. effusions in typical locations). CT study is still of paramount importance for the first evaluation of acute pancreatitis. Ultrasound could cover different roles during the course of the disease, because it could be used for short-term follow-up studies in the evaluation of possible complications and it could be used also to guide interventions [(4)].

Normal ultrasound findings can be seen in patients with interstitial edematous acute pancreatitis. Although the pancreas can appear normal in size and echopattern in a mild acute pancreatitis, the most frequent findings are focal or diffuse enlargement of the gland with a decrease of normal echogenicity, due to edema. Echogenicity of pancreatic parenchyma usually is lower compared to the liver, and the pancreatic echopattern may also

appear heterogeneous [Figure 7]. Acute pancreatitis can be focal or diffuse depending on its distribution [(18)] [Table 1].

Figure 7 Acute edematous pancreatitis: pancreatic parenchyma is heterogeneous with focal hypoechoic areas and a small effusion within the lesser sac (arrows).

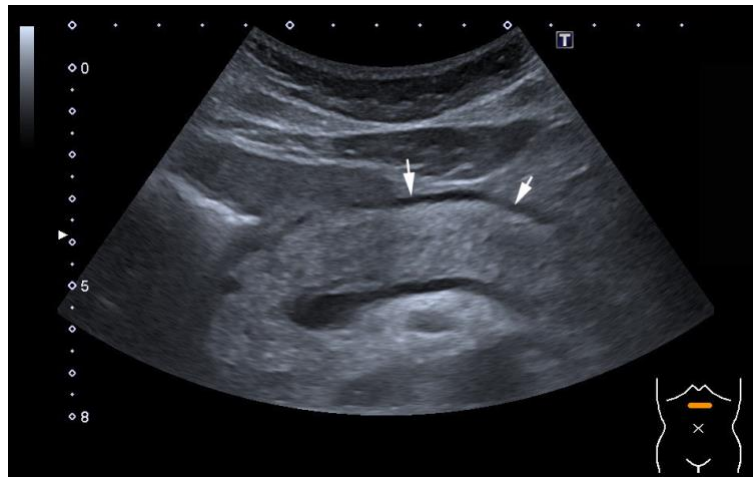


Table 1 Sonographic findings in acute pancreatitis.

Direct criteria	Indirect criteria
Increased diameter of the pancreas (whole pancreas, parts)	Fluid collections in typical locations (e.g. perisplenic, pararenal, Morissons pouch, pericolic, interenteric)
Inhomogeneous echopattern	Paralytic small intestine
Diffuse or focal hypoechoicity (edema)	Left pleural effusion
Hypoechoic focal mass lesion (hypervascular with CEUS)	
Peripancreatic fluid collections	

In acute necrotizing pancreatitis parts of the pancreas can be destroyed and liquefied, showing hypo-anechoic portions at ultrasound examination. A major problem of

conventional B-mode ultrasound is the detection of non-liquefied parenchymal necrosis because parenchymal vascularity cannot be assessed.

Acute peri-pancreatic fluid collections are anechoic [Figure 8]. Acute necrotic collections may be more heterogeneous due to the presence of echogenic debris within the fluid [Figure 9]. Acute fluid collections and acute necrotic collections occur most commonly around the pancreas and usually spread into both the lesser sac and the anterior para-renal space up to the peri-colic region [Figure 10] [(4)].

Figure 8 Acute peri-pancreatic fluid collection in acute pancreatitis (lesser sac).

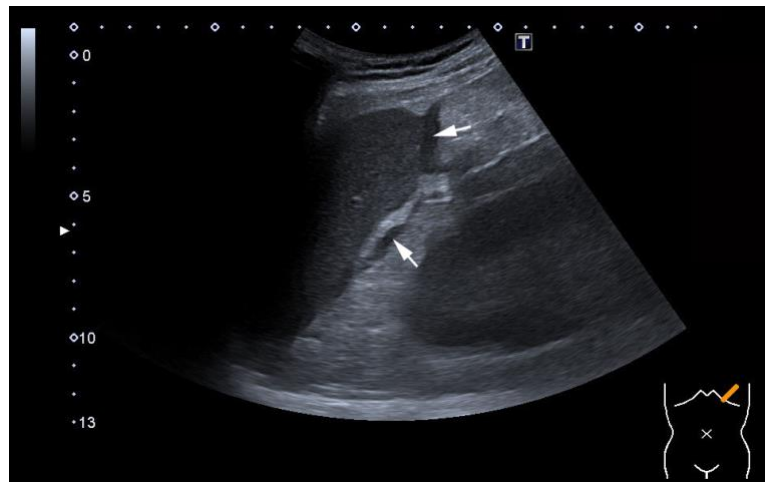


Figure 9 Acute necrotic collection in acute pancreatitis (lesser sac): note the echogenic debris within the collection.



Figure 10 Acute fluid collections in acute pancreatitis (arrows) in typical localisations: perisplenic (a) and surrounding the left kidney (b)

a



b



The role of transabdominal ultrasound in acute pancreatitis includes the search for gallstones as a possible etiology of pancreatitis. Moreover, the examiner should look for complications, e.g. intestinal paralysis, pancreatic ascites, necrotic collections, and thrombosis of the splanchnic veins.

Due to the inflammatory changes, in acute pancreatitis the consistency of the pancreatic parenchyma becomes softer than the healthy pancreas. This phenomenon may be evaluated using strain elastography or shear wave elastography, including ARFI. Necrosis can be identified at elastography as soft areas for the presence of damaged tissue with specific colors linked to softness [(8)].

On contrast-enhanced ultrasound (CEUS) the pancreatic segment involved in interstitial edematous acute pancreatitis shows an increased contrast-enhancement owing to hyperaemia. Conversely, necrotizing pancreatitis is characterised by the presence of large confluent necrotic areas. CEUS improves the identification and delimitation of these necrotic areas, which appear non-enhancing (avascular) at dynamic imaging [Figure 11] [(19;20)].

Figure 11: Acute necrotizing pancreatitis. B-Mode ultrasound shows a heterogeneous pancreatic body and acute peri-pancreatic fluid collections (a, arrows; * a small cyst of the pancreatic neck, which turned out to be a small intraductal papillary mucinous neoplasia of the side branch type). After injection of the ultrasound contrast agent

SonoVue® a large vascular necrosis of the complete pancreatic body is unmasked. Only the pancreatic head and the pancreatic capsule are enhancing. (b).

a



b



Pseudocysts are seen at ultrasound as a sharply delineated and anechoic lesions with distal acoustic enhancement, and they are typically oval or round. In contrast, walled off necrosis are delimited fluid collections with necrosis and debris inside, seen as echogenic particles within anechoic collections. Both typically show an enhancing wall at CEUS, with avascular fluids and debris inside.

Chronic pancreatitis

Chronic pancreatitis is an inflammatory disease characterised by the replacement of the pancreatic glandular elements by fibrous tissue. It is clinically characterised by a progressive

pancreatic functional loss [(21)]. Diagnosis of chronic pancreatitis is based on clinical findings, laboratory values of endocrine and exocrine pancreatic function, and imaging findings. Although early morphological changes of chronic pancreatitis are difficult to recognise at imaging, the findings of advanced disease are easily detected.

Alterations in size of the pancreas can be seen in less than half of patients affected by chronic pancreatitis [(22;24)]. Atrophy and focal alterations in pancreatic size are the most easily identified changes and are an expression of advanced stages. The glandular contours appear irregular, sharp and sometimes lumpy. Usually it could be seen a volume reduction of the gland, due to the chronic inflammatory process.

Echogenicity of the pancreas is usually increased in chronic pancreatitis owing to adipose infiltration [(25)] and fibrosis [(26-28)]; however, due to the presence of lipomatosis and fibrosis also in elderly and obese patients increased echogenicity is not a specific parameter of chronic pancreatitis. On the other hand, alterations of the parenchymal echopattern are a more specific sign of chronic pancreatitis. In patients with chronic pancreatitis, the parenchymal echopattern is inhomogeneous and coarse owing to the coexistence of hyperechoic and hypoechoic foci, fibrosis and inflammatory signs [(26;28)]. These findings are described in 50–70% of cases [(23;24)]. In patients affected by severe exocrine pancreatic insufficiency this percentage increases to approximately 80% [(22)], thus the presence of parenchymal inhomogeneity has a fairly good sensitivity for chronic pancreatitis with exocrine insufficiency. On the other hand, normal pancreatic echopattern is reported in the literature in up to 40% of cases of chronic pancreatitis and is observed especially in the early stages of the disease [(23;29-31)]. However, state-of-the-art ultrasound imaging (in particular using high-frequency and matrix transducers) has good capabilities for identifying also fine alterations of glandular texture (as honeycombing) present in the early stages of the disease.

The most important diagnostic criterion for chronic pancreatitis is the presence of pancreatic calcifications [(32)], whose identification is pathognomonic. At ultrasound they are identified as hyperechoic spots with posterior shadowing. However, very small calcifications may be difficult to detect. Diagnosis can be improved by the use of the so-called twinkling artefact. Twinkling artefact is characterized by a rapidly fluctuating mixture of Doppler signals that occurs behind a strongly reflecting granular interface such as pancreatic calcifications [(33)].

Moreover, the detection of pancreatic calcifications may be improved by the use of harmonic imaging and high resolution ultrasound [(4)].

Pancreatic duct calibre abnormalities in chronic pancreatitis are essentially represented by main pancreatic duct dilation.

The main pancreatic duct can be considered dilated when its calibre is larger than 3mm [(28)], with a sensitivity of approximately 60–70% [(24;25)] and a specificity of approximately 80–90% [(24;34;35)]. The only moderate sensitivity reflects the minor frequency of ductal dilation in initial and/or light cases of chronic pancreatitis. In the early phases of chronic pancreatitis the main pancreatic duct can have a normal diameter [(26)]. Compression of the main pancreatic duct may lead to secondary obstructive chronic pancreatitis upstream of the obstacle, with the same pathogenetic mechanism. Solid and cystic lesions may cause duct compression (benign) or infiltration (malignant) if contiguous to the main pancreatic duct, with progressive development of obstructive chronic pancreatitis upstream [(25)], making lots of difficulties in correct lesions detection and characterization. Therefore, in all cases of chronic pancreatitis, break-offs of a dilated pancreatic duct should be evaluated thoroughly in order to reveal the etiology of ductal stricture.

In conclusion, the most significant ultrasound findings in chronic pancreatitis are pancreatic duct dilation and intra-ductal calcifications. Obstruction of the common bile duct may occur [Figure 12, 13].

Due to the pathologic changes, the pancreatic tissue strain properties are different in respect to the healthy pancreas. A gland with chronic pancreatitis may show a wide range of tissue strain due to inhomogeneous distribution of pathological changes. Basically the elastogram shows harder pancreatic tissue and at qualitative elastography chronic pancreatitis is shown with heterogeneous mixed colored pattern or honeycombed pattern, with predominantly hard strands. Shear wave velocity in patients with chronic pancreatitis usually is significantly higher compared to healthy pancreas [(8)].

Figure 12 Chronic pancreatitis. Ultrasound oblique scan of the pancreatic gland shows main pancreatic duct dilation and calcifications. A large pancreatic stone is identified to be the cause of break-off of the dilated pancreatic duct.

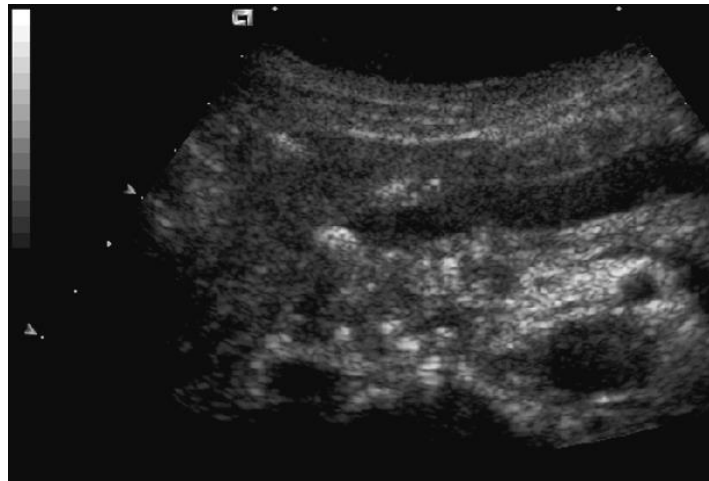


Figure 13 Chronic pancreatitis with stricture of the common bile duct (dilated common hepatic duct between markers; note the multiple calcifications of the enlarged pancreatic head).



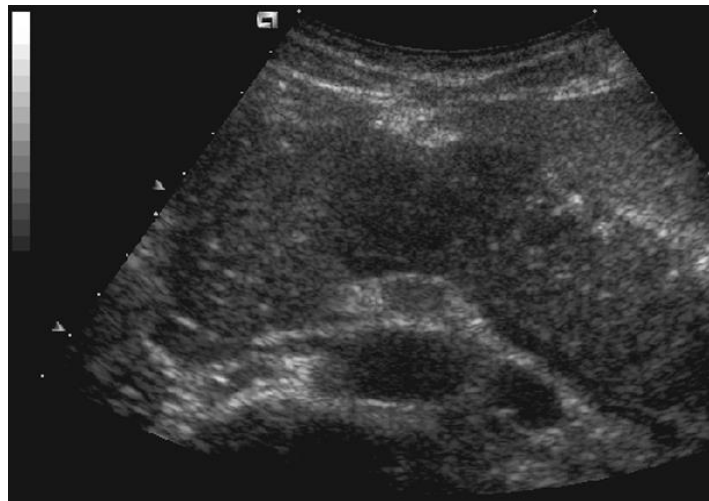
Autoimmune pancreatitis

Autoimmune pancreatitis is a rare cause of acute or chronic pancreatitis. It is characterised by peri-ductal inflammation, mainly sustained by lymphocytic infiltration, with evolution to

fibrosis. There are two main morphological types of autoimmune pancreatitis: focal and diffuse autoimmune pancreatitis. As opposed to other forms of chronic pancreatitis, the pancreas increases in volume, usually as a whole with the typical “sausage” aspect [Figure 14]. In diffuse autoimmune pancreatitis, the main pancreatic duct is compressed or string-like [(36)]. Ultrasound features include reduced echogenicity of the gland, diffuse or focal pancreatic enlargement, and the absence of any fluid collection or calcifications. The overall sensitivity of ultrasound in the diagnosis of autoimmune pancreatitis is variable, with an average range of 60–70% in most series [(21;22)]. The ultrasound features of focal autoimmune pancreatitis are less characteristic and very similar to those of mass-forming pancreatitis or pancreatic cancer; moreover if the disease is localized in the pancreatic head it could cause dilation of the common bile duct alone [(4;20)].

Figure 14 Autoimmune pancreatitis. (a) Ultrasound oblique scan of the pancreatic gland shows diffuse enlargement with the typical “sausage” aspect in absence of any fluid collection or calcification. (b) On contrast-enhanced ultrasound diffuse moderate enhancement is visible.

a



b



CEUS of autoimmune pancreatitis shows fair and moderate diffuse enhancement in the early contrast-enhanced phase, although it may be inhomogeneous [Figure 8]. Ultrasound contrast agent washout is usually slow but progressive. Therefore, CEUS is especially useful for the differentiation of focal forms of autoimmune chronic pancreatitis from pancreatic ductal adenocarcinoma, which is typically hypoenhancing [(37)]. Autoimmune chronic pancreatitis shows a remarkable response to steroid therapy because of its autoimmune pathogenesis [(38;39)].

Elastography might be helpful in patients with focal autoimmune pancreatitis due to the fact, that the characteristic stiff elastographic pattern in these patients is visible both in the lesion and in the adjacent pancreatic parenchyma [(8;40;41)].

Pancreatic focal inflammatory disease

Mass-forming pancreatitis

Mass-forming chronic pancreatitis usually occurs in patients with a history of chronic pancreatitis [(42)] and must be differentiated from pancreatic ductal adenocarcinoma. However, this differential diagnosis may be difficult due to the very similar ultrasound features [Figure 15]. In fact, both diseases can appear in most cases as hypoechoic masses, and also they may present with the same symptoms and signs. At ultrasound study the

presence of small calcifications within the lesion may suggest its inflammatory nature, but this sign is low in specificity [(4;43)].

Figure 15 Hypoechoic, ill-defined inflammatory pancreatic head tumor (T) in a case of “rim pancreatitis”. Differentiation from the duodenum (Duo, note the thickened hypoechoic wall) is not possible (a). The diameter of the common bile duct (CBD) is only slightly increased (b)

a



b



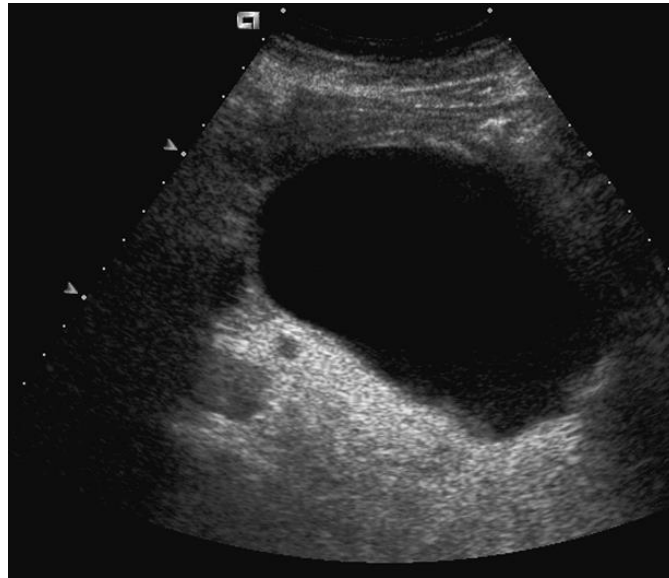
Biopsy or fine needle aspiration, guided by transabdominal ultrasound or endoscopic ultrasound, is often mandatory for a correct diagnosis. CEUS can improve the differential diagnosis between these two entities [(4;19)]. In particular, while ductal adenocarcinoma

remains hypoechoic in all contrast-enhanced phases, due to its intense desmoplastic reaction with poor mean vascular density of the lesion, the mass-forming chronic pancreatitis shows a “parenchymographic” enhancement, characterised by an enhancement pattern always comparable with that of the surrounding pancreatic parenchyma [(4;19;43)]. The CEUS finding consistent with an inflammatory origin is therefore the presence of parenchymal enhancement similar to that of the adjacent pancreas during the dynamic study. The intensity of this parenchymal enhancement is related to the length of the underlying inflammatory process. However, in long-standing chronic inflammatory processes, inhomogeneous hypovascularisation of the lesion may be observed with a less intense intralesional parenchymal enhancement, probably owing to the presence of a large amount of fibrosis, which means the differential diagnosis becomes more difficult [(19;43;44)]. As opposed to this, in more recent onset mass-forming pancreatitis the enhancement is usually more intense and prolonged [(4;45)].

Pseudocyst

Pseudocysts can be a complication (4 weeks after symptoms onset) of acute pancreatitis [Figure 16] or can occur in chronic pancreatitis [(37)]. They are characterised by a fibrous wall without an epithelial lining [(46)]. Pseudocysts must be differentiated from pancreatic cystic tumours, especially mucinous cystadenomas (MCAs), as they require completely different therapeutic approaches [(46)]: history of acute or chronic pancreatitis episodes helps in correct diagnosis and patients diagnostic overview. CEUS has a important role in differential diagnosis of pseudocysts and pancreatic cystic tumours through the better evaluation of the vascularization of the intralesional vegetations.

Figure 16 Pseudocyst. Ultrasound oblique scan of the pancreatic body shows a huge rounded cystic lesion after severe acute pancreatitis.



Walled off necrosis

The walled off necrosis (WON) can be another type of complication, that arises 4 weeks after symptoms onset of acute pancreatitis. They are characterized by chronic fluid collections with necrosis and debris inside, seen as echogenic particles within anechoic collections. After contrast injection at CEUS it typically shows an enhancing wall, with avascular fluids collected inside. All inclusions are completely avascular and therefore without any enhancement during CEUS examination [(43)].

Pancreatic solid neoplasm

Ductal adenocarcinoma

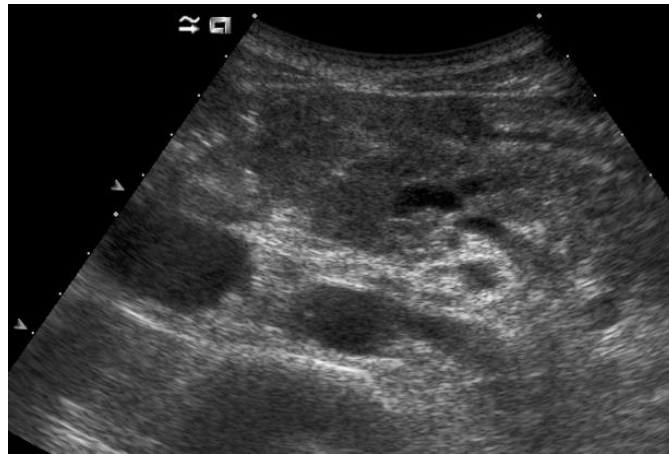
Approximately 90% of pancreatic tumours are ductal adenocarcinomas. They are composed of infiltrating epithelium resembling ductal structures. In almost two thirds of patients with pancreatic adenocarcinoma the tumour is located in the head of the pancreas; Body and/or tail are affected only in one third of patients. Diffuse infiltration is rare.

Ultrasound is often the non-invasive imaging method for the first evaluation of the pancreas. Since adenocarcinoma is the most common primary malignancy of the pancreas, each pancreatic solid mass detected at ultrasound has a high probability of being an adenocarcinoma, even if not every solid pancreatic mass detected at ultrasound is obviously an adenocarcinoma.

Macroscopically, ductal adenocarcinoma appears as a scirrhous infiltrating mass [(47–50)].

Masses in the head of the pancreas cause a ductal obstruction with secondary dilation of both the common bile duct and the main pancreatic duct, resulting in the so-called “double-duct sign”. However, “double-duct sign”.can also be present in chronic pancreatitis. In particularly aggressive forms of adenocarcinoma the development of necrosis or colliquation is common and results from the difference between the growth rate and the formation of microvessels by angiogenesis. The necrotic/fluid part of the tumour is mainly located centrally and may cause a cystic appearance of the lesion. A ductal adenocarcinoma is characterised by infiltration of the tumour into the adjacent parenchyma and structures. This feature could explain the common lack of clear-cut margins during examinations. Therefore, sometimes delineation of the mass is difficult, but may be improved using harmonic imaging and compound techniques [(4)]. Due to the very low US acoustic impedance of the tumor, pancreatic ductal adenocarcinoma nearly always presents as a solid and markedly hypoechoic mass compared to the adjacent pancreatic parenchyma [Figure 17].

Figure 17 Ductal adenocarcinoma. Ultrasound oblique scan of the pancreatic body shows hypoechoic mass with ill-defined infiltrative margins and upstream main pancreatic duct dilation.

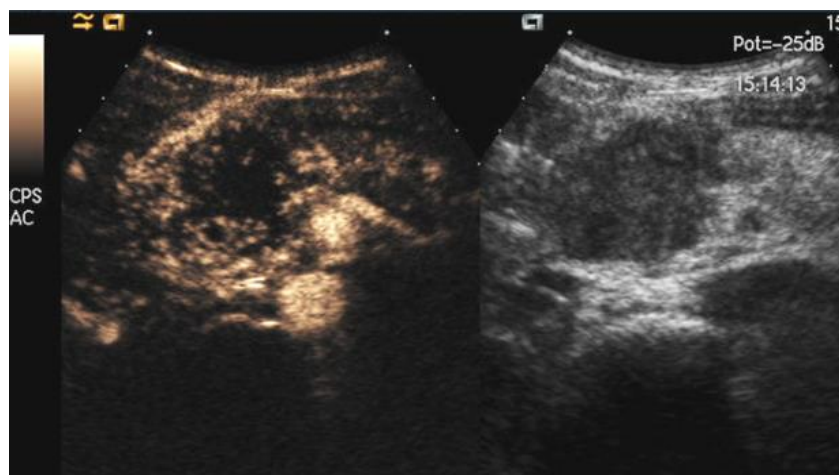


The main pancreatic duct is usually infiltrated and dilated upstream. Thus, the identification of duct dilation with abrupt cut-off has to be considered a secondary sign suspicious of pancreatic ductal adenocarcinoma. Moreover, due to the fact that the most common pancreatic tumor is ductal adenocarcinoma and most of them are localized in the cephalopancreatic region of the gland, a dilated pancreatic duct with abrupt cut-off is the most important sign for early detection even if the tumor itself cannot be visualized [(4;51)]. As a consequence, patients with unexplained dilatation of the pancreatic main duct with an abrupt cut-off should be referred to more specific imaging studies. Doppler studies show poor or no vascularity inside the lesion.

The ultrasound study must include adjacent vascular structures evaluation, mainly to distinguish between resectable and non-resectable ductal adenocarcinomas. The examiner should look for the echogenic fatty interface between tumor and adjacent vessels, their course and blood-flow. At conventional ultrasound, vascular invasion is defined by a focal absence of the echogenic interface of the vessel wall or by narrowing of the vessel lumen, with changes in blood flow velocity [(52-55)]. Principal criteria of unresectable pancreatic cancer are liver or peritoneal metastases and invasion of major peri-pancreatic arteries (celiac trunk, superior mesenteric artery, common hepatic artery) [(56)]. The introduction of ultrasound contrast agents has significantly strengthened ultrasound studies, increasing the

accuracy of the first line examination in the characterization of pancreatic tumors, especially pancreatic adenocarcinoma [(4;43;56-59)]. On CEUS, ductal adenocarcinoma enhancement is poor in all contrast-enhanced phases [Figure 18]. At CEUS ductal adenocarcinoma typically presents as a hypoenhancing mass compared to the adjacent parenchyma; this pattern was present in about 90% of cases in a multicentre study [(60)]. Therefore, CEUS reliably can characterize pancreatic ductal adenocarcinoma. In particular, every pancreatic solid hypoechoic mass detected at ultrasound, hypoenhancing in all phases at CEUS, has to be considered a ductal adenocarcinoma, until otherwise proven [(61)].

Figure 18 Ductal adenocarcinoma. Contrast-enhanced ultrasound transversal scan of the pancreatic head showing a markedly hypovascularised mass with upstream main pancreatic duct dilation.



The margins and size of the lesion are more clearly visible after contrast injection. The depiction of tumour margins at CEUS is more accurate at low enhancement of pancreatic adenocarcinoma [(59)]. In cases of well-differentiated pancreatic ductal adenocarcinoma, the mass tends to be isovascular compared with the remaining parenchyma and the margins of the tumour are no longer visualised. The relationship with peri-pancreatic arterial and venous vessels can also be evaluated for local staging. The particular grade of differentiation of the adenocarcinoma influences the microvascular density [(43;44;59;62)]. Moreover, the pattern of enhancement of pancreatic adenocarcinoma influences the depiction of tumoural margins at CEUS [(59)]. CEUS quantitative perfusion analysis of pancreatic ductal

adenocarcinoma could give quantitative evaluation of the enhancement, allowing a more objective characterization of the tumor [(63)].

Following the study of a pancreatic lesion during the arterial, pancreatic and venous phases, the presence of liver metastases has to be excluded during the late phase [(43)]. As a consequence, the evaluation of the whole liver at CEUS is mandatory after the pancreatic study. The late phase, 120 seconds after bolus injection, is the best phase for the detection of metastatic liver lesions and each solid hypoechoic focal liver lesion detected during the late phase should be considered a metastasis until otherwise proven [(4;58;64;65)]. Since ultrasound is often the first technique performed, the use of CEUS will improve the diagnostic accuracy when a focal hypoechoic solid lesion has been detected.

Due to its pathology, pancreatic ductal adenocarcinoma is a hard hypovascular mass, so usually malignant pancreatic neoplasms, have harder stiffness than adjacent pancreatic parenchyma at elastographic. Pancreatic ductal adenocarcinoma usually presents at qualitative and quantitative elastography as a harder mass than normal adjacent pancreatic parenchyma; it is also usually harder than benign lesions, but this last feature is not always very simple to appreciate at elastographic studies [(8)].

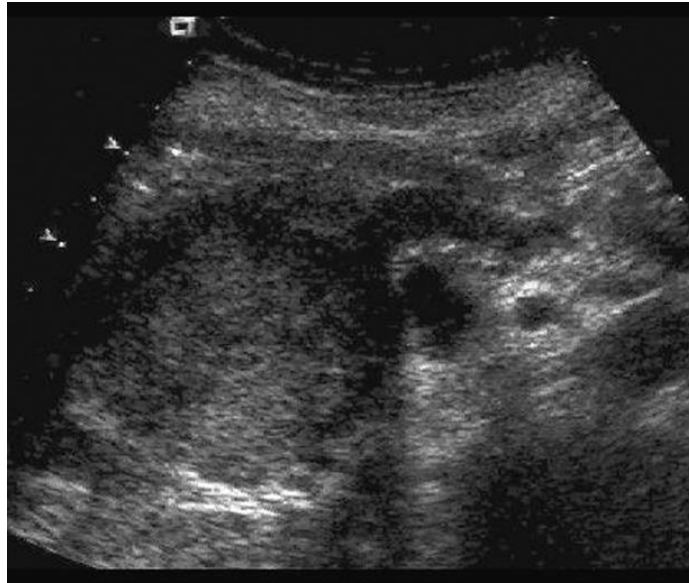
Neuroendocrine tumours

Pancreatic neuroendocrine tumours or islet cell tumours arise from the neuroendocrine cells of the pancreas. These tumours are classified as functioning or non-functioning, based on the presence or absence of symptoms related to hormone production. Insulinomas and gastrinomas are the most common functioning islet cell tumours and they are usually small at the time of diagnosis. The other functioning neuroendocrine tumours (vipoma, glucagonoma and somatostatinoma) are rare, bigger and they usually have a more malignant behaviour in respect to insulinomas and gastrinomas; they account for approximately 20% of functioning neuroendocrine tumours of the pancreas [(66;67)]. Non-functioning tumours are frequently large at diagnosis [Figure 19] and are often malignant [(68)].

Figure 19 Neuroendocrine tumour (non-functioning). (a) Ultrasound transversal scan of the pancreatic head shows large hypoechoic mass with well-defined margins and

upstream main pancreatic duct dilation. (b) The lesion is hypervascular at contrast-enhanced ultrasound.

a



b



Insulinomas are usually benign and solitary pancreatic lesions (they can be multifocal in patients with MEN1 syndrome), while gastrinomas tend to be malignant and multiple. Insulinomas represent the most frequently found functioning neuroendocrine tumours of the pancreas (approximately 60% of all neuroendocrine tumours). They are benign (85–99%) and single (93–98%) in the majority of cases [(69;70)]. Insulinoma appears as hypoechoic

pancreatic nodule, is usually capsulated and has a mean diameter between 0.5 and 2 cm. In fact at clinical presentation 50% of the tumours are smaller than 1.5cm and therefore are often very difficult to depict [(67)]. The diameter of malignant insulinoma is generally greater than 3 cm with approximately a third having metastases at the time of diagnosis [(69;70)]. At ultrasound they usually appear as a small, well-defined, and encapsulated homogeneously hypoechoic nodule with hyperenhancement at CEUS [Figure 12] [(61;71)]. Sometimes, very small calcifications can be present, especially in larger lesions. The preoperative ultrasound detection of small insulinomas can sometimes be very difficult. Gastrinomas are the second most frequently found functioning neuroendocrine tumour of the pancreas (approximately 20% of all neuroendocrine tumours) [(66;67)].

These tumours differ from insulinomas in localisation and size [(66;72;73)]. They occur within the gastrinoma triangle (the junction of the cystic duct and common bile duct, junction of the second and third parts of the duodenum, junction of the head and neck of the pancreas), of which it is only possible to explore the pancreatic side by ultrasound [(66;67)]. Due to their larger size, detection of pancreatic gastrinomas is more easy compared to insulinomas [(67;73)]. Liver metastases are present in 60% of cases at the time of diagnosis [(67;74)]. They could be multifocal in a bigger percentage of cases (around 20%), often when they present in MEN1 syndrome. Gastrinoma usually presents as a homogeneous hypoechoic mass [(55)].

Glucagonomas, VIPomas, somatostinomas, and serotoninomas are rare. Usually they are larger than insulinomas, often have a malignant behaviour and tend to metastasize early.

Non-functioning pancreatic neuroendocrine tumours represent up to 33% of all neuroendocrine tumours of the pancreas [(75)] and range from 1–20cm in diameter. They have a high malignancy rate of up to 90% [(75;76)]; however, they are less aggressive than adenocarcinomas, and the differential diagnosis between these two entities is very important due to the different therapeutic approaches. These tumours, characterised by predominantly expansive growth in contrary to ductal adenocarcinomas are not clinically apparent until adjacent viscera and structures have become involved. On ultrasound they appear well-delineated and are usually easy to detect because of their size. Owing to their dimensions, necrosis and haemorrhage may be present; they develop a typical inhomogeneous appearance and are sometimes accompanied by very small intralesional calcifications. Larger non-functioning pancreatic neuroendocrine tumours show cystic

degeneration or cystic changes [(66)]. Numerous intratumoral vascular spots are a typical finding of neuroendocrine pancreatic tumours on colour Doppler. In particular, a “spotted” pattern can be demonstrated in both large and small endocrine tumours [(66)]. However, while positive Doppler results predict hypervascularisation of the lesion, a Doppler “silence” can also be present in hypervascular neuroendocrine tumours because of the small size of the tumoural vascular network.

On CEUS, different enhancement patterns can be observed in relation to the size of the tumours and tumoural vessels. Voluminous neuroendocrine tumours show a rapid and intense enhancement in the early contrast-enhanced phase [Figure 13], with the exception of necrotic intralesional areas [(66;77;78)]. In small to moderate-sized neuroendocrine pancreatic tumours, a capillary blush enhancement can be present in the early contrast-enhanced phase, mirroring the most characteristic angiographic feature of these tumors, which becomes hypoechoic in the late contrast-enhanced phase [(66;77;78)].

Non-functioning neuroendocrine tumours can also be hypovascularised, depending on the amount of stroma inside the lesion, which is dense and hyalinised [(37)].

The high capability of CEUS to show pancreatic tumor vascularity is the result of the high resolution of ultrasound imaging, combined with the size and the blood-pool distribution of the microbubbles contrast material [(61)]. Summarizing, there is convincing evidence that CEUS can be a useful tool to improve the characterization of pancreatic neuroendocrine tumors and their differentiation from pancreatic ductal adenocarcinoma [(77)].

At elastographic studies pancreatic neuroendocrine tumors tend to be harder than the adjacent pancreatic parenchyma, but usually less stiff than ductal adenocarcinoma [(8)].

Lymphoma

Primary pancreatic lymphoma is a rare pancreatic neoplasm; the secondary involvement of the pancreas by non-Hodgkin’s B-cell lymphoma is more common and can occur in 30–40 % of patients with extranodal disease.

Different radiological appearances of primary pancreatic lymphoma have been described: the well-circumscribed nodular type with solitary pancreatic mass (most common appearance); diffuse type with pancreatic enlargement; peripheral lymphomatous involvement, mimicking autoimmune pancreatitis; and multinodular type. When primary pancreatic lymphoma presents as a solitary pancreatic mass, it has to be differentiated from

ductal adenocarcinoma, because is frequently heterogeneous, large and it can extend and infiltrate beyond the gland, also encasing major peri-pancreatic vessels. However, the degree of main pancreatic duct dilation is minimal even with ductal invasion: this lesser degree of ductal dilatation it is an important sign and should raise the suspicion of a pancreatic lymphoma.

Diffuse infiltration and enlargement of the pancreas, without clinical signs of acute pancreatitis, and with lymph nodes enlargement and systemic symptoms, should alert to the possibility of a pancreatic lymphoma [(61;79)].

Ultrasound shows focal or diffuse pancreatic enlargement, which is hypoechoic relative to the normal pancreatic parenchyma [(55)].

Metastases

Pancreatic metastases are rare. Primary tumours that frequently metastasize to the pancreas originate from the lung, breast, kidney and melanoma [(80)]. Pancreatic metastases can appear as focal or multifocal lesions or may present with a diffuse pancreatic involvement. When metastases present as nodules, they are often well-demarcated lesions in patients with a known primary neoplasm [(55)].

Pancreatic metastases should be included in the differential diagnosis of primary pancreatic neoplasms, such as ductal adenocarcinoma and neuroendocrine tumors. Usually pancreatic metastases from renal cell carcinoma or from melanoma are clearly hypervascular, with typical enhancement at CEUS. Therefore, they have to be differentiated from neuroendocrine tumors (exhibiting similar enhancement patterns) based on clinical history, symptoms, and finally on cytology. Whereas other pancreatic hypovascular metastases have to be differentiated from pancreatic ductal adenocarcinoma [(81;83)].

Pancreatic cystic neoplasm

Serous cystadenoma

Serous pancreatic neoplasms are cystic tumors, usually detected in middle age (50–60-years) women (F:M = 2:1) as solitary lesions. The most common serous pancreatic neoplasm is the

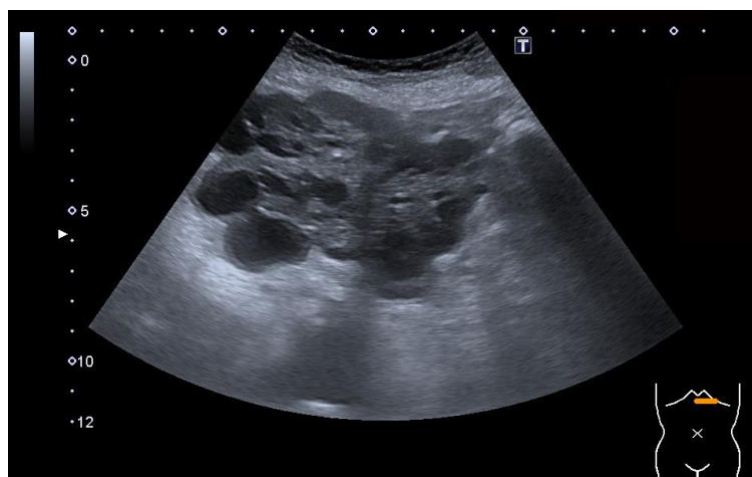
serous cystadenoma (SCA). These kinds of lesions are typical of patients with von Hippel–Lindau disease, where they can be more often multifocal.

Serous cystadenoma is a benign lesion, usually located in the head of the pancreas [(46)].

Typically it presents as a solitary multilocular microcystic lesion with a honeycomb architecture (microcystic type), because of the presence of multiple microcysts (<20 mm), thin wall, and thin multiple septa oriented toward the centre of the lesion [(84)], without communication with the pancreatic ductal system. In up to 15% of cases, the tumour contains a central scar, which may calcify. If extremely microcystic, SCA can have a solid appearance on ultrasound and CT, resembling a neuroendocrine pancreatic tumor after contrast agent administration, owing to the homogeneous hyperenhancement of the extremely compacted internal septa [(55)], but it has a typical cystic appearance at MRI. Other types of serous cystadenoma are the macrocystic type and the oligocystic type: Differentiation from other macrocystic tumours of the pancreas, in particular mucinous cystic neoplasms, is very difficult.

The content of the cysts is glycogen-rich serous, so it is anechoic at ultrasound. The typical microcystic type (70% of cases) has a cloud-like morphology, clearly shown by ultrasound, characterized by lobulated contours with thin walls and a “honeycomb” multilocular architecture due to the presence of anechoic microcysts (≤ 20 mm), separated by thin internal septa, centrally oriented. These numerous thin septa with radial arrangement give the lesion its typical microcystic aspect [Figure 20].

Figure 20 Giant serous cystic neoplasm of the pancreatic body with solid appearing echogenic parts and middle-sized cysts



The central scar, if present, is fibrovascular, visible as a central solid echogenic portion of the tumour, which sometime calcifications, and a vessel within it can be visualized at color-Doppler imaging [(55;61)].

SCAs do not communicate with the main pancreatic duct, but may cause compression and upstream dilatation. Lack of ductal communication is crucial for the differentiation of SCA from intraductal papillary mucinous neoplasms (IPMN) of the branch-duct type, but may be very difficult to be demonstrated at ultrasound [55].

At contrast enhanced ultrasound, enhancement of intralesional septae improves the identification of the microcystic features of the lesion. The central scar, when present, shows a homogeneous enhancement [27;28]. At elastographic study, the serous content of SCA implicates mosaic pattern and non-numerical values at the quantitative ultrasound elastographic study made by ARFI imaging [(8)].

Mucin producing neoplasms

Mucin producing neoplasms of the pancreas may originate either from the peripheral ducts (mucinous cystic tumour) or from the main pancreatic duct and its side branches (intraductal papillary mucinous neoplasms, IPMNs) [(85)].

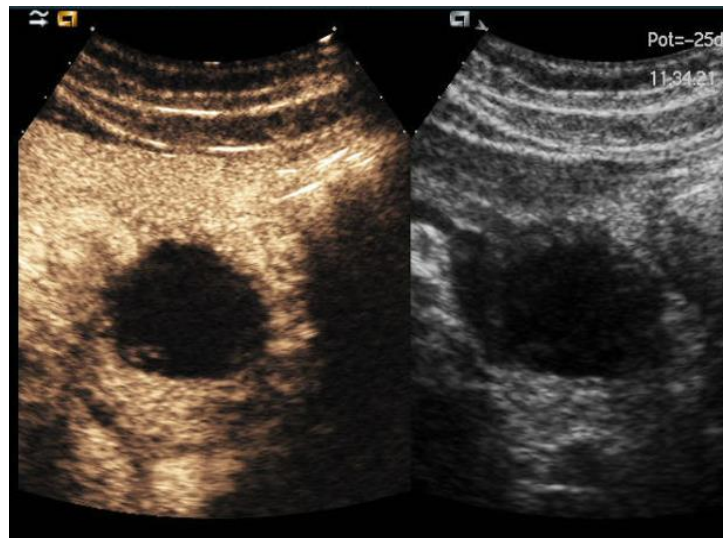
Mucinous cystadenoma

Mucinous cystic neoplasms (MCN) are thick-walled, uni- or multilocular tumors composed of mucin-containing cysts. These neoplasms occur almost exclusively in women (F:M = 9:1) and are mainly located in the body and/or tail of the pancreas. These neoplasms encompass a spectrum of lesions from benign, such as mucinous cystadenoma (MCA), to invasive and potentially metastasizing mucinous cystadenocarcinoma, and they always require surgical resection [(86;87)]. MCA usually presents as a unilocular or oligolocular (≤ 6 cysts) cystic lesion, with a rounded ball-like morphology. There is no connection with the pancreatic main duct. On ultrasound, it appears as round or ovoid unilocular lesion with a thick wall and septa and occasionally peripheral calcifications. The mucinous content is viscous and may generate fine echoes in the internal part of the lesion, making the lesion heterogeneously hypoechoic at US. Moreover MCA may include internal septa and/or solid papillary

projections. The detection of vascularized vegetations is fundamental for the differential diagnosis between MCN and pseudocyst. The number and the thickness of intralesional septa and nodules are not always related to the grade of malignancy.

CEUS may significantly improve the ultrasonographic detection and identification of parietal nodules and septa, mainly detecting their vascularization. The vascularisation of septa and nodules can be demonstrated using a hyperechoic beam [Figure 21]. Owing to its special technical features, as the dynamic evaluation of perfusion by using a blood pool contrast agent, CEUS can sometimes better demonstrate the enhancement of septa and nodules than other imaging studies. Moreover, owing to the deletion of background tissues and of all the echogenic intra-cystic content (mucin, clots, or debris), the detection rate of septa and nodules at CEUS is absolutely superior as compared to B-mode ultrasound, improving the characterization of cystic tumors; in fact, as previously said, at unenhanced ultrasound, the mucin viscosity causes an increased echogenicity, which can obscure internal septa or nodules [(61)]. CEUS examination therefore improves ultrasonographic differential diagnosis between MCA and pseudocysts, as a result of the identification and study of vascularisation of intracystic structures [(88;89)]. The presence of enhanced mural nodules is closely related to the risk of malignancy and should raise the suspicion of transformation to cystadenocarcinoma. All mucin producing tumours are filled with complex fluid. As a consequence, at ARFI quantitative imaging it is reasonable to expect number values of shear waves, contrary to what happens with serous neoplasms [(8)].

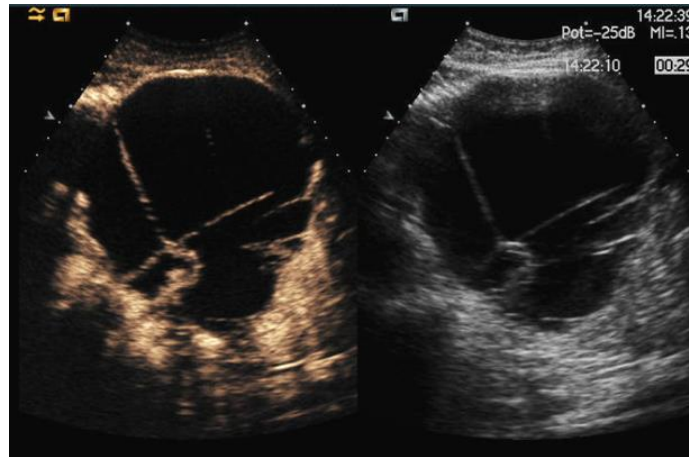
Figure 21 Mucinous cystadenoma. Ultrasound oblique scan of the pancreatic body shows rounded cystic mass with small enhancing septa.



Mucinous cystadenocarcinoma

Mucinous cystadenocarcinoma represents the malignant neoplastic transformation of mucinous cystadenoma. Compared with the latter it is characterised by thicker wall and septa, inhomogeneous content and a greater number of mural nodules [Figure 22], whose significant cell proliferation is responsible for wall and then peripheral structure invasion, leading to lymph nodes involvement and liver metastases development [(86;87)]. As previously stated, CEUS is able to accurately demonstrate the enhancement of neoplastic vegetations within the tumor, helping moreover in the differentiation among neoplastic vegetations of viable tissue and echogenic intra-cystic content, such as mucin, clots, or debris, composed by not viable tissue. Moreover quantitative perfusion analysis of the CEUS enhancement can reveal higher perfusion values in the site of neoplastic degeneration [(4;90)].

Figure 22 Mucinous cystadenocarcinoma. Ultrasound oblique scan of the pancreatic body shows huge rounded cystic mass with thick wall and several enhancing septa and nodules.



Intraductal papillary mucinous neoplasm

Intraductal papillary mucinous neoplasm (IPMN) is a group of exocrine mucin-producing tumors, with common presentation in males with a mean age of 60 years old. In particular related to improvements in imaging quality, the incidence and the incidental detection of these neoplasms has increased in the recent years. IPMN is recognised as a cystic dilation of the main pancreatic duct and/or its branches with proliferation of pancreatic ductal epithelium and excessive production of mucin. IPMNs are divided in three types [(91)]: the main duct type, with a segmental or diffuse main pancreatic duct dilation, without any abrupt cut-off of the duct; the branch duct type, appearing as unilocular or multilocular cystic lesions with variable diameter from few millimeters to some centimeters separated by thin septa, uni- or multi-focal, with grape-like clusters uni- or multifocal; and the mixed type, affecting both the main duct and its side-branches [(4;92;93)]. The localised main duct type of IPMN is characterised by highly inhomogeneous masses, related to neoplastic intraductal proliferation, with upstream dilation of the main pancreatic duct. The diffuse main type may be difficult to distinguish from chronic pancreatitis. The branch duct mucinous tumour is characterised by cystic ectasia of one or more branches, which form masses. The demonstration of the involvement or the communication with the main pancreatic duct is essential for an appropriate diagnosis. The segmental or diffuse involvement of the main pancreatic duct characterizes lesions with higher risk of malignancy. In particular, a main pancreatic duct with a diameter larger than 10 mm is highly suggestive of malignancy. Other

reported features of malignancy are based on the presence of peripheral or septal calcification, the presence of enhanced mural nodules, enhanced solid mass in the dilated main duct or within the cystic lesions, thick septa, and enhanced ductal wall [(4;94;95)]. At ultrasound, IPMN usually appears as a complex hypoechoic indefinite mass with dilation of the main pancreatic duct if involved. In side branch type IPMN connection to the pancreatic ductal system often is not visible on transabdominal ultrasound. Typically side branch type IPMN appears as a s multilocular grape-like cystic lesions [Figure 23].

Figure 23 Large multilocular cystic lesion of the pancreatic body, which was diagnosed to be a side branch type of IPMN using endoscopic ultrasound.



On ultrasound examination the mucin of IPMN may not be easily differentiated from the solid portions of the tumour, which can therefore be mistakenly reported as solid. Harmonic imaging, with its better contrast resolution, may lead to better identification of the non-solid part of the lesion because of the demonstration of more or less sharp intralesional interfaces, improving ultrasound accuracy [(96;97)]. However, on ultrasound, final diagnosis of IPMN by demonstrating the communication with the pancreatic duct is difficult [(98)]. Moreover, ultrasound fails in correct evaluation of the number of lesion, which is very important for further management. IPMN of the branch-duct type in up to two thirds of cases presents multifocally.

The correct technique for the ultrasound evaluation of a cystic pancreatic lesion requires the use of contrast agent injection as reported in the 2011 EFSUMB guidelines [(65)]. As

reported for other pancreatic cystic tumors, the enhancement of internal vegetations sometimes can be better demonstrated at CEUS than on other imaging modalities, thanks to the real-time evaluation and the high spatial resolution. CEUS examination of the IPMNs can allow identification of intraductal papillary tumoural vegetations, by demonstrating its vascularisation. CEUS can be a safe method to follow-up borderline lesions by evaluating changes in dimensions and vascularisation of the inclusion. In this setting, CEUS has the significant advantage of being a non-invasive and low-cost technique [(83)].

At imaging, characteristics of malignancy are local invasion signs, vascular encasement or infiltration, peri-pancreatic lymph nodes enlargement and distant spread.

The international consensus guidelines recommend resection for all main-duct IPMNs and for branch-duct IPMNs with features highly suggestive for malignancy (“high-risk stigmata”). For asymptomatic branch-duct IPMNs measuring less than 3 cm careful observations is recommended in the absence of solid components or substantial main duct dilation [(4;99)].

Solid pseudopapillary tumor

Solid pseudopapillary tumours (SPTs) are rare epithelial neoplasms with low malignant potential that occur predominantly in young women (85-90%), in the second to fourth decades. These tumours have a highly variable appearance from completely solid tumors to almost completely cystic masses. Smaller lesions are usually totally or predominantly solid, while larger lesions generally present as large well-encapsulated masses with variable solid and cystic components due to a haemorrhagic degeneration [(61)].

At ultrasound examination solid pseudopapillary tumour is usually a well-encapsulated lesion with cystic and solid components, but sometimes the mass is completely solid, appearing as a hypoechoic mass with well-defined margins, especially in lesions of small size. Internal septa or calcifications may be observed. Typically, there is no upstream ductal dilatation.

At CEUS, solid pseudopapillary tumours typically show a rim enhancement, with non-enhancing areas inside the lesions, compatible with necrotic or haemorrhage portions. This rim enhancement is related to the presence of a pseudocapsule of compressed normal pancreatic adjacent parenchyma. The lesions appear to be iso- or hypoenhancing, compared to the normal parenchyma during all the examination phases [(4;100)].

Other imaging modalities: which, who, why when?

The characterisation of solid and cystic pancreatic tumours can be improved by the complimentary use of different imaging modalities, such as B-Mode ultrasound, CEUS, endoscopic ultrasound (EUS), CT and MRI.

Usually, at least in Europe, an ultrasound study could be the first imaging evaluation in patients with abdominal symptoms. For these reasons is very important for the sonographer to have good knowledge about ultrasound features of different pancreatic diseases and, last but not least, about appropriate diagnostic and therapeutic management.

Following ultrasound detection of a focal pancreatic lesion, the immediate injection of ultrasound contrast agents is a relatively new, safe and feasible technique allowing for better characterization and staging of the lesion during the same examination. CEUS facilitated a more accurate differentiation between solid and cystic lesions, hyper-enhancing, hypo-enhancing and un-enhancing lesions, so influencing the choice of further examinations. Moreover, a faster diagnosis can be obtained [(55;57)].

In case of solid pancreatic lesion at ultrasound examination, the patient could be referred for a CT evaluation for further characterization and staging. However, approximately 30% of ductal adenocarcinoma smaller than 2 cm (too small for causing early secondary signs) are isodense in the arterial phase of the CT study [(101)]. In cases with a definite ultrasound finding of a solid pancreatic lesion with a negative result of CT imaging, MRI and/or EUS are indicated due to the high sensitivity of both techniques in demonstrating small-sized ductal adenocarcinomas. Basically, an MRI study should be preferred over CT for further evaluation of pancreatic nodules smaller than 2 cm detected at ultrasound. D'Onofrio et al. reported a high sensitivity of B-Mode ultrasound and CEUS in diagnosing pancreatic ductal adenocarcinoma, with no significant difference compared to contrast-enhanced CT. Therefore, combining B-Mode ultrasound and CEUS with contrast-enhanced CT could increase imaging diagnostic performance and may allow an earlier diagnosis of ductal adenocarcinoma [(102)].

In case of cystic pancreatic lesions, the best imaging method for further evaluation is MRI, due to its capability to show fluids components within lesions. Moreover, magnetic resonance cholangiopancreatography (MRCP) is highly sensitive for demonstration or exclusion of ductal communication of pancreatic cystic neoplasms. In case of absolute

contraindications to MRI, patients could undergo CT, but it is important to underline that this imaging method has lower ability in showing cystic lesions features. Current guidelines recommend EUS (optionally with fine-needle aspiration) for further evaluation of cystic pancreatic neoplasms with worrisome features on radiological imaging.

According to the Italian consensus guidelines [(103)] conventional ultrasound of the pancreas is not able to definitively diagnose cystic pancreatic neoplasms, whereas the different dynamic imaging modalities (CEUS, contrast enhanced CT, MRI) have a similar high accuracy. Contrast enhanced CT and MRI are the best imaging modalities for differentiating mucinous and non-mucinous neoplasms, both having high accuracy. In fact, MRI and contrast enhanced CT are first level techniques in differentiating benign from malignant cystic pancreatic neoplasms. The performance of CEUS is similar to that of MRI and contrast enhanced CT, when cystic pancreatic neoplasms are visible at ultrasound. MRI with MRCP is the best imaging modality for evaluating the communication of cystic pancreatic neoplasms with the main pancreatic duct, with the results that MRI with MRCP is the imaging method of choice for the study of cystic pancreatic neoplasms. However, it is important to remember that also CEUS favorably compares with MRI in displaying the anatomic features of the cystic pancreatic masses and is highly sensitive in the detection of the vascularization of the cystic inclusions, such as septa and nodules [(104)]. Only in case of ambiguous imaging findings fine needle aspiration (FNA) is indicated. There are no data supporting the role of percutaneous image-guided sampling of cystic pancreatic neoplasms. The FNA of cystic pancreatic neoplasms has to be performed using EUS-guidance. Moreover, EUS can identify morphological features which increase the suspicion of malignancy in cystic lesions. However, morphologic features identified at EUS alone cannot exclude the presence of malignancy in these neoplasms. Although EUS morphology alone cannot provide a definite differential diagnosis between mucinous and non-mucinous cystic pancreatic neoplasms, some EUS features offer useful information on the type of lesion, helping by contrast agents injection in ruling out neoplastic degeneration.

References

1. Rumack C, Wilson SR, Charboneau JW. Diagnostic ultrasound. New York: Mosby Year Book 1991; 145–177.

2. Mittelstaedt CA. Abdominal ultrasound. New York: Mosby 1987; 163–176.
3. Martínez-Noguera A, D’Onofrio M. Ultrasonography of the pancreas. 1. Conventional imaging *Abdom Imaging* 2007; 32(2):136-149.
4. D’Onofrio M (ed) (2012) Ultrasonography of the pancreas. Imaging and pathological correlations. Springer Verlag Italia.
5. Hohl C, Schmidt T, Honnef D, et al. Ultrasonography of the pancreas. 2. Harmonic Imaging. *Abdom Imaging*, 2007; 32:150-60.
6. Hohl C, Schmidt T, Haage P, et al. Phase-inversion tissue harmonic imaging compared with conventional Bmode ultrasound in the evaluation of pancreatic lesions. *Eur Radiol*, 2004; 14:1109-17.
7. Desser TS, Jeffrey RB. Tissue harmonic imaging techniques: physical principles and clinical applications. *Semin Ultrasound CT MR*, 2001; 22:1-10.
8. Clevert D, D’Onofrio M, Quiaia E (eds). Atlas of elastosonography. Clinical applications with imaging correlations. Springer Verlag Italia, 2017.
9. Janssen J, Schlorer E, Greiner L. EUS elastography of the pancreas: feasibility and pattern description of the normal pancreas, chronic pancreatitis, and focal pancreatic lesions. *Gastrointest Endosc*. 2007; 65:971–8.
10. Gallotti A, D’Onofrio M, Pozzi Mucelli R. Acoustic radiation force impulse (ARFI) technique in ultrasound with virtual touch tissue quantification of the upper abdomen. *Radiol Med*. 2010; 115:889–97.
11. Hakimé A, Giraud M, Vullierme MP, Vilgrain V. MR imaging of the pancreas. *J Radiol*; 2007, 88:11-25.
12. Debi U, Kaur R, Prasad KK, et al. Pancreatic trauma: a concise review. *World J Gastroenterol*, 2013; 19(47): 9003-11.
13. Miele V, Piccolo CL, Galluzzo M, et al. Contrast-enhanced ultrasound (CEUS) in blunt abdominal trauma. *Br J Radiol*, 2016; 89(1061): 20150823.
14. Catalano O, Lobianco R, Sandomenico F, et al. Real-time, contrast-enhanced sonographic imaging in emergency radiology. *Radiol Med*, 2004; 108: 454-69.
15. Lenhart DK, Balthazar EJ. MDCT of acute mild (necrotizing) pancreatitis: abdominal complications and fate of fluid collections. *AJR Am J Roentgenol*, 2008; 190: 643-649.
16. Sarr MG, Banks PA, Bollen TL, et al. Revision of the Atlanta classification of acute pancreatitis. Acute Pancreatitis Classification Workgroup, April 2008.

<http://www.pancreasclub.com/resources/AtlantaClassification>. Accessed October 2, 2017

17. Weissleder R, Rieumont MJ, Wittenberg J Primer of diagnostic imaging. 2nd ed. New York: Mosby Year Book 1997; 220–228.
18. Lorén I, Lasson A, Fork T, et al. New sonographic imaging observations in focal pancreatitis. *Eur Radiol* 1999; 9:862–867.
19. D’Onofrio M, Zamboni G, Tognolini A, Malagò R, Faccioli N, Frulloni L, Pozzi Mucelli R. Mass-forming pancreatitis: value of CEUS. *World J Gastroenterol* 2006; 12:4181–4184.
20. Numata K, Ozawa Y, Kobayashi N, Kubota T, Akinori N, Nakatani Y, Sugimori K, Imada T, Tanaka K. Contrast-enhanced sonography of autoimmune pancreatitis: comparison with pathologic findings. *J Ultrasound Med* 2004; 23:199–206.
21. Freeny P, Lawson T. Radiology of the pancreas. New York: Springer-Verlag 1982, 449.
22. Bolondi L. Sonography of chronic pancreatitis. *Radiol Clin North Am* 1989; 27:815–833.
23. Alpern MB, Sandler MA, Kellman GM, Madrazo BL. Chronic pancreatitis: ultrasonic features. *Radiology* 1985; 155:215–219.
24. Bolondi L, Priori P, Gullo L, et al. Relationship between morphological changes detected by ultrasonography and pancreatic exocrine function in chronic pancreatitis. *Pancreas* 1987; 2:222–229.
25. Lankisch PG, Banks PA Chronic pancreatitis: etiology. In: Lankisch PG, Banks PA (eds) *Pancreatitis*. New York: Springer Verlag 1998; 199–208.
26. Lecesne R, Laurent F, Drouillard J, et al. Chronic pancreatitis. In: Baert AL, Delorme G, Hoe L Van (eds) *Radiology of the pancreas*. 2nd rev ed. New York: Springer Verlag 1999; 145–180.
27. Husband JE, Meire HB, Kreel L. Comparison of ultrasound and computer tomography in pancreatic diagnosis. *Br J Radiol* 1977; 50:855–863.
28. Remer EM, Baker MB. Imaging of chronic pancreatitis. *Radiol Clin N Am* 2002; 40:1229–1242.
29. Lees WR, Vallon AD, Denyer ME, et al. Prospective study of ultrasonography in chronic pancreatic disease. *BMJ* 1979; 1:162–164.
30. Foley WD, Stewart ET, Lawson TL, et al. Computer tomography, ultrasonography and echoscopic retrograde cholangiopancreatography in the diagnosis of pancreatic disease: a comparative study. *Gastrointestinal Radiol* 1980; 5:29–35.

31. Grant TH, Efrusy ME. Ultrasound in the evaluation of chronic pancreatitis. *JAMA* 1981; 81:183–188.
32. Homma T, Harada H, Koizumi M. Diagnostic criteria for chronic pancreatitis by the Japan Pancreas Society. *Pancreas* 1997; 15:14–15.
33. Kim HC, Yang DM, Jin W, et al. Color Doppler twinkling artifacts in various conditions during abdominal and pelvic sonography. *J Ultrasound Med*, 2010; 29:621-32.
34. Niederau C, Grendell JH. Diagnosis of chronic pancreatitis. *Gastroenterology* 1985; 88:1973–1995.
35. Hessel ST, Siegelman SS, McNeil BJ, et al. A prospective evaluation of computer tomography and ultrasound of the pancreas. *Radiology* 1982; 143:129–133.
36. Furukawa N, Muranaka T, Yasumori K, et al. Autoimmune pancreatitis: radiologic findings in three histologically proven cases. *J Comput Assist Tomogr* 1998; 22:880–883.
37. Faccioli N, Crippa S, Bassi C, D'Onofrio M. Contrast-enhanced ultrasonography of the pancreas. *Pancreatology*. 2009; 9(5):560-6.
38. Okazaki K. Autoimmune-related pancreatitis. *Curr Treat Options Gastroenterol* 2001; 4:369–375.
39. Kamisawa T, Yoshiike M, Egawa N, Nakajima H, Tsuruta K, Okamoto A. Treating patients with autoimmune pancreatitis: results from a long-term follow-up study. *Pancreatology* 2005; 5:234–240
40. Mondal U, Henkes N, Patel S, et al. Endoscopic ultrasound elastography. Current clinical use in pancreas. *Pancreas*. 2016; 45:929–33.
41. Dietrich CF, Hirche TO, Ott M, et al. Real-time tissue elastography in the diagnosis of autoimmune pancreatitis. *Endoscopy*. 2009; 41:718–20.
42. Kim T, Murakami T, Takamura M, Hori M, Takahashi S, Nakamori S, Sakon M, Tanji Y, Wakasa K, Nakamura H. Pancreatic mass due to chronic pancreatitis: correlation of CT and MR imaging features with pathologic findings. *AJR Am J Roentgenol* 2001; 177:367-371.
43. D'Onofrio M, Zamboni G, Faccioli N, Capelli P, Pozzi Mucelli R. Ultrasonography of the pancreas. 4. Contrast enhanced imaging. *Abdom Imaging* 2007; 32:171-181.
44. Takeda K, Goto H, Hirooka Y, Itoh A, Hashimoto S, Niwa K, Hayakawa T. Contrast-enhanced transabdominal ultrasonography in the diagnosis of pancreatic mass lesions. *Acta Radiol* 2003; 44:103-106.

45. Rickes S, Unkrodt K, Neye H, et al. Differentiation of pancreatic tumours by conventional ultrasound, unenhanced and echo-enhanced power Doppler sonography. *Scand J Gastroenterol*, 2002; 37:1313-20.
46. Procacci C, Biasiutti C, Carbognin G, Capelli P, El-Dalati G, Falconi M, Misiani G, Ghirardi C, Zamboni G. Pancreatic neoplasms and tumor-like conditions. *Eur Radiol* 2001; 11Suppl2:S167-S192.
47. Cubilla AI, Fitzgerald PJ. Tumors of the esocrine pancreas. 2nd Series. Ed. Washington, DC: Armed Forces Institute of Pathology 1984.
48. O' Connor TP, Wade TP, Sunwoo YC, et al. Small cell undifferentiated carcinoma of the pancreas. Report of a patient with tumor marker studies. *Cancer* 1992; 70:1514-1519.
49. Tryka AF, Brooks JR. Histopathology in the evaluation of total pancreatectomy for ductal carcinoma. *Ann Surg* 1979; 190:373-381.
50. Yeo CJ, Cameron JL, Lillemoe KD, et al. Pancreaticoduodenectomy for cancer of the head of the pancreas. 201 patients. *Ann Surg* 1995; 221:721-733.
51. Tanaka S, Nakao M, Ioka T, et al. Slight dilatation of the main pancreatic duct and presence of pancreatic cysts as predictive signs of pancreatic cancer: a prospective study. *Radiology*, 2010; 254:965-972.
52. Bertolotto M, D'Onofrio M, Martone E, Malagò R, Pozzi Mucelli R. Ultrasonography of the pancreas. 3. Doppler imaging. *Abdom Imaging* 2007; 32:161-170.
53. Koito K, Namieno T, Nagakawa T, Hirokawa N, Ichimura T, Syonai T, Yama N, Someya M, Nakata K, Sakata K, Hareyama M. Pancreas: imaging diagnosis with color/power Doppler ultrasonography, endoscopic ultrasonography, and intraductal ultrasonography. *Eur J Radiol* 2001; 38:94-104.
54. Ueno N, Tomiyama T, Tano S, Wada S, Miyata T. Color Doppler ultrasonography in the diagnosis of portal vein invasion in patients with pancreatic cancer. *J Ultrasound Med* 1997; 16:825-830.
55. Martínez-Noguera A, D'Onofrio M. Ultrasonography of the pancreas. 1. Conventional imaging *Abdom Imaging* 2007; 32(2):136-149.
56. D'Onofrio M, Zamboni G, Malagò, R et al. Resectable pancreatic adenocarcinoma: is the enhancement pattern at contrast-enhanced ultrasonography a pre-operative prognostic factor? *Ultrasound Med Biol*, 2009; 35:1929-193712.

57. D'Onofrio, Martone E, Malagò R, et al. Contrast-enhanced ultrasonography of the pancreas. *JOP*, 2007; 8[S1]:71-76.
58. Claudon M, Cosgrove D, Albrecht T, et al. Guidelines and good clinical practice recommendations for contrast enhanced ultrasound (CEUS) - update 2008. *Ultraschall Med*, 2008; 29:28-44.
59. Faccioli N, D'Onofrio M, Malagò R, Zamboni G, Falconi M, Capelli P, Mucelli RP. Resectable pancreatic adenocarcinoma: depiction of tumoral margins at CEUS. *Pancreas* 2008; 37:265–268.
60. D'Onofrio M, Barbi E, Dietrich CF, et al. Pancreatic multicenter ultrasound study (PAMUS). *Eur J Radiol*, 2011; 81(4): 630-8.
61. D'Onofrio M, Capelli P, Pederzoli P, editors. *Imaging and pathology of pancreatic neoplasms. A pictorial atlas*. Italia: Springer; 2015.
62. Oshikawa O, Tanaka S, Ioka T, Nakaizumi A, Hamada Y, Mitani T. Dynamic sonography of pancreatic tumors: comparison with dynamic CT. *AJR Am J Roentgenol* 2002; 178:1133–1137.
63. D'Onofrio M, Canestrini S, Crosara S, et al. Contrast enhanced ultrasound with quantitative perfusion analysis for objective characterization of pancreatic ductal adenocarcinoma: a feasibility study. *World J Radiol*, 2014; 6(3): 31-5.
64. D'Onofrio M, Martone E, Faccioli N, et al. Focal liver lesions, sinusoidal phase of CEUS. *Abdom Imaging*, 2006; 31:529-536.
65. Piscaglia F, Nolsøe C, Dietrich CF, et al. The EFSUMB Guidelines and Recommendations on the Clinical Practice of Contrast Enhanced Ultrasound (CEUS): Update 2011 on non-hepatic applications. *Ultraschall Med* 2012;33(1):33-59).
66. D'Onofrio M, Mansueto GC, Falconi M, Procacci C. Neuroendocrine pancreatic tumor: value of contrast enhanced ultrasonography. *Abdom Imaging* 2004; 29:246–258.
67. Ros PR, Morteale KJ. Imaging features of pancreatic neoplasms. *JBR-BTR* 2001; 84(6):239–249.
68. Buetow PC, Miller DL, Parrino TV. Islet cell tumors of the pancreas: clinical, radiologic, and pathologic correlation in diagnosis and localization. *Radiographics* 1997; 17:453–472.
69. Liu TH, Tseng HC, Zhu Y. Insulinoma. An immunohistochemical and morphologic analysis of 95 cases. *Cancer* 1985; 56:1420–1429.

70. Stefanini P, Carbonni M, Patrassi N. Beta islet-cell tumors of the pancreas: result of a study on 1067 cases. *Surgery* 1974; 75:597.
71. Dixon E, Pasiaka JL. Functioning and nonfunctioning neuroendocrine tumors of the pancreas. *Curr Opin Oncol*, 2007; 19:30–35.
72. Pereira PL, Wiskirchen J. Morphological and functional investigations of neuroendocrine tumors of the pancreas. *Eur Radiol* 2003; 13(9):2133–2146.
73. Semelka RC, Cumming MJ, Shoenut JP, Magro, et al. Islet cell tumors: comparison of dynamic contrast-enhanced CT and MR imaging with dynamic gadolinium enhancement and fat suppression. *Radiology* 1993; 186(3):799–802.
74. Mergo PJ, Helmberger TK, Buetow PC, et al. Pancreatic neoplasm: MR imaging and pathologic correlation. *Radiographics* 1997; 17:281–301.
75. Fugazzola C, Procacci C, Bergamo Andreis IA, Iacono C, et al. The contribution of ultrasonography and computed tomography in the diagnosis of nonfunctioning islet cell tumors of the pancreas. *Gastrointest Radiol* 1990; 15(2):139–144.
76. Eckhauser FE, Cheung PS, Vinik AI, et al. Nonfunctioning malignant neuroendocrine tumors of the pancreas. *Surgery* 1986; 100:978–988.
77. Malagò R, D’Onofrio M, Zamboni GA, Faccioli N, Falconi M, Boninsegna L, Mucelli RP. Contrast-enhanced sonography of nonfunctioning pancreatic neuroendocrine tumors. *AJR Am J Roentgenol* 2009; 192:424–430.
78. D’Onofrio M, Malagò R, Zamboni G, Vasori S, Falconi M, Capelli P, Mansueto G. CEUS better identifies pancreatic tumor vascularization than helical CT. *Pancreatology* 2005; 5:398–402.
79. Merkle EM, Bender GN, Brambs HJ. Imaging findings in pancreatic lymphoma: differential aspects. *AJR Am J Roentgenol*, 2000; 174(3):671–5.
80. Merkle EM, Braz T, Kolkythas O, et al. Metastases to the pancreas. *Br J Radiol* 1998; 71:1208–1214.
81. Flath B, Rickes S, Schweigert M, Lochs H, Possinger K, Wermke W. Differentiation of a pancreatic metastasis of a renal cell carcinoma from a primary pancreatic carcinoma by echo-enhanced power Doppler sonography. *Pancreatology* 2003; 3:349-351.
82. Megibow AJ. Secondary pancreatic tumors: imaging. In: Procacci C, Megibow A, editors. *Imaging of the pancreas: cystic and rare tumors*. Berlin: Springer-Verlag 2003; 277-288.

83. D'Onofrio M, Megibow AJ, Faccioli N, Malagò R, Capelli P, Falconi M, Mucelli RP. Comparison of contrast-enhanced sonography and MRI in displaying anatomic features of cystic pancreatic masses. *AJR Am J Roentgenol* 2007; 189:1435–1442.
84. Kim YH, Saini S, Sahani D, et al. Imaging diagnosis of cystic pancreatic lesions: pseudocyst versus non-pseudocyst. *Radiographics*, 2005; 25(3):671–85.
85. Procacci C, Graziani R, Bicego E, et al. Intraductal mucinproducing tumors of the pancreas: imaging findings. *Radiology* 1996; 198:249–257
86. Tham RT, Heyerman HG, Falke TH, et al. Cystic fibrosis: MR imaging of the pancreas. *Radiology* 1991; 179:183–186.
87. Ros PR, Hamrick-Turner JE, Chiechi MV, et al. Cystic masses of the pancreas. *Radiographics* 1992; 12:673–686.
88. D'Onofrio M, Caffarri S, Zamboni G, Falconi M, Mansueto G. CEUS in the characterization of pancreatic mucinous cystadenoma. *J Ultrasound Med* 2004; 23: 1125–1129.
89. D'Onofrio M, Zamboni G, Malago` R, Martone E, Falconi M, Capelli P, Mansueto G. Pancreatic pathology. In: Quaia E (ed) *Contrast media in ultrasonography*. Springer-Verlag: Berlin 2005; 335–347.
90. Xu M, Xie XY, Liu GJ, et al. The application value of contrast-enhanced ultrasound in the differential diagnosis of pancreatic solid-cystic lesions. *Eur J Radiol*, 2011; 81(7): 1432-7.
91. Procacci C, Megibow AJ, Carbognin G, et al. Intraductal papillary mucinous tumor of the pancreas: a pictorial essay. *Radiographics* 1999; 19:1447–1463.
92. Fukukura Y, Fujiyoshi F, Sasaki M, et al. Intraductal papillary mucinous tumors of the pancreas. *Am J Roentgeno*, 2000; 174:441-44.
93. Sahani DV, Kadavigere R, Saokar A, et al. Cysticpancreatic lesions: a simple imaging-based classification system for guiding management. *Radiographics*, 2005; 25:1471-84.
94. Ishida M, Egawa S, Aoki T, et al. Characteristic clinic-pathological features of the types of intraductal papillary-mucinous neoplasms of the pancreas. *Pancreas*, 2007; 35:348-52.
95. Guarise A, Faccioli N, Ferrari M, et al. Evaluation of serial changes of pancreatic branch duct intraductal papillary mucinous neoplasms by follow-up with magnetic resonance imaging. *Cancer Imaging*, 2008; 8:220-8.
96. Shapiro RS, Wagreich J, Parsons RB, et al. Tissue harmonic imaging sonography: evaluation of image quality compared with conventional sonography. *AJR* 1998; 171:1203-1206.

97. Bennett GL, Hann LE. Pancreatic ultrasonography. *Surg Clin North Am* 2001; 81:259–281.
98. Procacci C, Schenal G, Dalla Chiara E, et al. Intraductal papillary mucinous tumors: imaging. In: Procacci C, Megibow AJ (eds) *Imaging of the pancreas cystic and rare tumors*. Berlin: Springer Verlag 2003; 97–137.
99. Tanaka M, Chari S, Adsay V, et al. International consensus guidelines for management of intraductal papillary mucinous neoplasms and mucinous cystic neoplasms of the pancreas. *Pancreatology*, 2006; 6:17-32.
100. Coleman KM, Doherty MC, Bigler SA. Solid pseudopapillary tumor of the pancreas. *Radiographics*, 2003; 23:1644-8.
101. Yoon SH, Lee JM, Cho JY, et al. Small (≤ 2 cm) pancreatic adenocarcinomas: analysis of enhancement patterns and secondary signs with multiphasic multidetector CT. *Radiology* 2011; 259(2): 442-52.
102. D'Onofrio M, Crosara S, Signorini M, et al. Comparison between CT and CEUS in the diagnosis of pancreatic adenocarcinoma. *Ultraschall Med*, 2013; 34: 377-81.
103. Italian association of hospital gastroenterologist and endoscopists; Italian association for the study of the pancreas, Buscarini E, Pezzilli R, Cannizzaro R, et al. Italian consensus guidelines for the diagnostic work-up and follow-up of cystic pancreatic neoplasms. *Dig Liver Dis*, 2014; 46(6): 479-93.
104. D'Onofrio M, Megibow AJ, Faccioli N, et al. Comparison of contrast-enhanced sonography and MRI in displaying anatomic features of cystic pancreatic masses. *AJR American journal of roentgenology*, 2007; 189: 1435-42.